PHYSICAL REVIEW B **90**, 140507(R) (2014)

$SrPt_3P$: A two-band single-gap superconductor

R. Khasanov,[1,*] A. Amato,[1] P. K. Biswas,[1] H. Luetkens,[1] N. D. Zhigadlo,[2] and B. Batlogg[2]
[1]*Laboratory for Muon Spin Spectroscopy, Paul Scherrer Institute, CH-5232 Villigen PSI, Switzerland*
[2]*Laboratory for Solid State Physics, ETH Zurich, 8093 Zurich, Switzerland*

(Received 22 April 2014; revised manuscript received 8 October 2014; published 28 October 2014)

The magnetic penetration depth (λ) as a function of applied magnetic field and temperature in $SrPt_3P$ ($T_c \simeq 8.4$ K) was studied by means of muon-spin rotation (μSR). The dependence of λ^{-2} on temperature suggests the existence of a single s-wave energy gap with the zero-temperature value $\Delta_0 = 1.55(2)$ meV. At the same time λ was found to be strongly field dependent which is the characteristic feature of the nodal gap and/or multiband systems. The multiband nature of the superconducting state is further suggested by the upward curvature of the upper critical field. This apparent contradiction is resolved by $SrPt_3P$ being a particular two-band superconductor with equal gaps but different coherence lengths within the two Fermi surface sheets.

DOI: 10.1103/PhysRevB.90.140507 PACS number(s): 74.72.Gh, 74.25.Jb, 74.25.Op, 76.75.+i

After the discovery of the first Fe-based superconductors enormous efforts were made to improve their superconducting properties. The intensive search led to the discovery of several Fe-based materials (see, e.g., Ref. [1] for review and references therein) and related compounds such as $BaNi_2As_2$ [2], $SrNi_2As_2$ [3], $SrPt_2As_2$ [4], and SrPtAs [5], without Fe and relatively low superconducting transition temperatures T_c's.

Recently, Takayama *et al.* [6] reported the synthesis of a new family of ternary platinum phosphide superconductors with the chemical formula APt_3P (A = Sr, Ca, and La) and T_c's of 8.4, 6.6, and 1.5 K, respectively. Theoretical studies on the pairing mechanism in these new compounds gave partially contradicting results [7,9]. The authors of Ref. [7] performed first-principles calculations and proposed that superconductivity is caused by the proximity to a dynamical charge-density wave instability, and that a strong spin-orbit coupling leads to exotic pairing in at least $LaPt_3P$. In contrast, the first-principles calculations and Migdal-Eliashberg analysis performed by Subedi *et al.* [9] suggest conventional phonon-mediated superconductivity. Also experimentally seemingly contradicting results were obtained. Based on the observation of nonlinear temperature behavior of the Hall resistivity, the authors of Ref. [6] suggest multiband superconductivity in these new compounds. Note that the presence of two bands crossing the Fermi level was indeed revealed by *ab initio* band structure calculations presented in [7,9–11]. On the other hand the specific-heat data of $SrPt_3P$ were found to be well described within a single-band, single s-wave gap approach with the zero-temperature gap value of $\Delta_0 = 1.85$ meV [6].

In this Rapid Communication we report on the results of muon-spin rotation (μSR) studies of the magnetic penetration depth (λ) as a function of temperature and magnetic field of the novel superconductor $SrPt_3P$. Below $T \simeq T_c/2$ the superfluid density ($\rho_s \propto \lambda^{-2}$) becomes temperature independent which is consistent with a fully gapped superconducting state. The full temperature dependence of $\rho_s(T)$ is well described within a single s-wave gap scenario with the zero-temperature gap value $\Delta_0 = 1.55(2)$ meV. On the other hand, λ was found to increase with increasing magnetic field as is observed in multiband superconductors or superconductors with nodes in the energy gap function. The upper critical field shows a pronounced upward curvature thus pointing to a multiband nature of the superconducting state of $SrPt_3P$. Our results indicate that $SrPt_3P$ is a two-band superconductor with equal gaps but different coherence length parameters ξ_i for the two Fermi surface sheets.

The sample preparation and the magnetization experiments were performed at the ETH-Zürich. Polycrystalline samples of $SrPt_3P$ were prepared using the cubic anvil high-pressure and high-temperature technique. Coarse powders of Sr, Pt, and P elements of high purity (99.99%) were weighed according to the stoichiometric ratio 1:3:1, thoroughly ground, and enclosed in a boron nitride container, which was placed inside a pyrophyllite cube with a graphite heater. All procedures related to the sample preparation were performed in an argon-filled glove box. In a typical run, a pressure of 2 GPa was applied at room temperature. While keeping the pressure constant, the temperature was ramped up in 2 h to the maximum value of 1050 °C, maintained for 20–40 h, and then decreased to room temperature in 1 h. Afterward, the pressure was released, and the sample was removed. All high-pressure prepared samples demonstrate large diamagnetic response with the superconducting transition temperature of $\simeq$8.4 K (see the inset in Fig. 1). The powder x-ray diffraction patterns are consistent with those reported in Ref. [6].

Measurements of the upper critical field B_{c2} were performed using a Quantum Design 7 T SQUID magnetometer. The temperature dependence of B_{c2} was obtained from field-cooled magnetization curves [$M_{FC}(T)$] measured in constant magnetic fields ranging from 0.3 mT to 4 T (see Fig. 1 and Sec. S1 in the Supplemental Material [8]). The $B_{c2}(T)$ curve exhibits a pronounced upward curvature around ~6–6.5 K. Linear fits of $B_{c2}(T)$ in the vicinity of T_c and for $T \leqslant 6$ K yield $dB_{c2}/dT = -0.49$ and -0.77 T/K, respectively. Open circles correspond to $B_{c2}(T)$ data points from Ref. [6]. They are in perfect agreement with our data thus implying that the upturn on $B_{c2}(T)$ reported here is indeed a generic property of the $SrPt_3P$ compound. Note that an upward curvature of $B_{c2}(T)$ was also observed previously for a number of materials such as Nb [12,13], V [12], $NbSe_2$ [14–16], MgB_2 [17–19], borocarbides and nitrides [20–22], heavy

*rustem.khasanov@psi.ch

RAPID COMMUNICATIONS

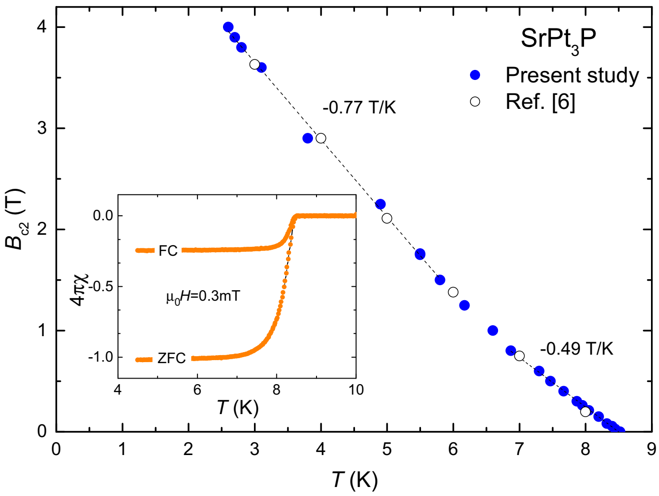

FIG. 1. (Color online) The temperature dependence of the upper critical field B_{c2} of $SrPt_3P$ (closed circles). The dotted lines are linear fits of $B_{c2}(T)$ in the vicinity of T_c and for $T \leqslant 6$ K. Open circles are $B_{c2}(T)$ data points from Ref. [6]. The inset shows the temperature dependence of the zero-field-cooled (ZFC) and field-cooled (FC) magnetization measured at $\mu_0 H = 0.3$ mT.

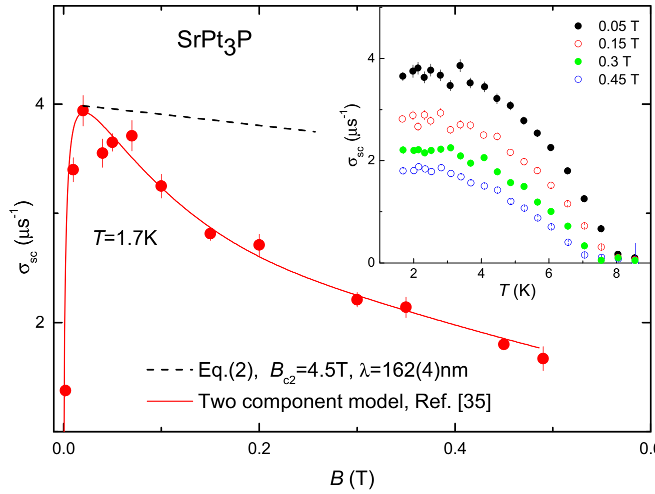

FIG. 2. (Color online) The dependence of the depolarization rate σ_{sc} on the applied field B at $T = 1.7$ K. The dashed black line represents $\sigma_{sc}(B)$ as expected within the model of Brandt [34] for $\lambda = 162(4)$ nm and $B_{c2} = 4.5$ T obtained in magnetization experiments. The red solid line is the fit by means of the two-component model from Ref. [35] with the parameters $\xi_1 = 8.6$ nm, $\xi_2 = 26$ nm, $\lambda = 134(2)$ nm, and $w = 0.72(2)$; see Sec. S2 in the Supplemental Material [8]. The inset shows the temperature dependence of the depolarization rate σ_{sc} caused by the formation of FLL in $SrPt_3P$ in fields of 0.05, 0.15, 0.3, and 0.45 T.

fermion systems [23], and various iron-based [24–26] and cuprate superconductors [27,28], and was often associated with two-band superconductivity.

The temperature and the magnetic field dependence of the magnetic penetration depth λ were obtained from transverse-field (TF) μSR data [29]. The experiments were carried out at the $\pi E1$ beam line at the Paul Scherrer Institute (Villigen, Switzerland). The data were analyzed using the free software package MUSRFIT [30]. In a polycrystalline sample the magnetic penetration depth λ can be extracted from the Gaussian muon-spin depolarization rate $\sigma_{sc}(T) \sim \lambda^{-2}$, which reflects the second moment ($\sigma_{sc}^2/\gamma_\mu^2$, γ_μ is the muon gyromagnetic ratio) of the magnetic field distribution due to the flux-line lattice (FLL) in the mixed state [31–33]. The TF-μSR data were analyzed using the asymmetry function

$$A(t) = A_{sc}\exp\left[-\left(\sigma_{sc}^2 + \sigma_n^2\right)t^2/2\right]\cos(\gamma_\mu B_{sc} t + \phi)$$
$$+A_b \exp\left(-\sigma_b^2 t^2/2\right)\cos(\gamma_\mu B_b t + \phi). \qquad (1)$$

The first term of Eq. (1) represents the response of the superconducting part of the sample. Here A_{sc} denotes the initial asymmetry; σ_{sc} is the Gaussian relaxation rate due to the FLL; σ_n is the contribution to the field distribution arising from the nuclear moment and which is found to be temperature independent, in agreement with the ZF results (not shown); B_{int} is the internal magnetic field sensed by the muons and ϕ is the initial phase of the muon-spin ensemble. The second term with the initial asymmetry A_b, small $\sigma_b < 0.3\ \mu s^{-1}$ and B_b close to the applied field corresponds to the background muons stopping in the cryostat and in nonsuperconducting parts of the sample.

Figure 2 shows the evolution of σ_{sc} at $T = 1.7$ K as a function of the applied magnetic field B. Each data point was obtained after cooling the sample in the corresponding field from above T_c to 1.7 K. The overall decrease of σ_{sc} with increasing applied field is partially caused by the decreased width of the internal field distribution upon approaching B_{c2}. To quantify such an effect, one can make use of the numerical Ginzburg-Landau model, developed by Brandt [34]. This model predicts the magnetic field dependence of the second moment of the magnetic field distribution, i.e., the μSR depolarization rate:

$$\sigma_{sc}\ [\mu s^{-1}] = 4.83 \times 10^4 (1 - B/B_{c2})$$
$$\times[1 + 1.21(1 - \sqrt{B/B_{c2}})^3]\lambda^{-2}\ [\mathrm{nm}^{-2}]. \qquad (2)$$

Under the assumption of field-independent λ the dependence of σ_{sc} on B was analyzed by using the values of the upper critical field B_{c2} as obtained in magnetization experiments [$B_{c2}(1.7)$ K $\simeq 4.5$ T, see Fig. 1]. It is clear that the theoretical $\sigma(B)$, which is presented in Fig. 2 by the dashed line, is not in agreement with the data.

The dependence of σ_{sc} on B was further analyzed using the two-component model proposed by Serventi *et al.* [35]. The model considers the independent contributions of two bands. Each band is characterized by its own coherence length (ξ_1, ξ_2), while the parameter $w_1 = \rho_{s,1}/\rho_s$ accounts for the contribution of the first band into the total superfluid density (see Ref. [35] and Sec. S2 in the Supplemental Material [8]). The results of the fit with $\lambda = 134(2)$ nm, $w = 0.72(2)$, $\xi_1 = 8.6$ nm, and $\xi_2 = 26$ nm are presented in Fig. 2 by the solid red line.

The temperature dependences of λ^{-2} for $\mu_0 H = 0.05, 0.15,$ 0.3, and 0.45 T were obtained from measured $\sigma_{sc}(T)$'s (the inset in Fig. 2) and $B_{c2}(T)$ (Fig. 1) using Eq. (2). Figure 3 shows $\lambda^{-2}(T)$ normalized to its value averaged over the temperature range 1.7–3.5 K as a function of $T/T_c(B)$. All data curves

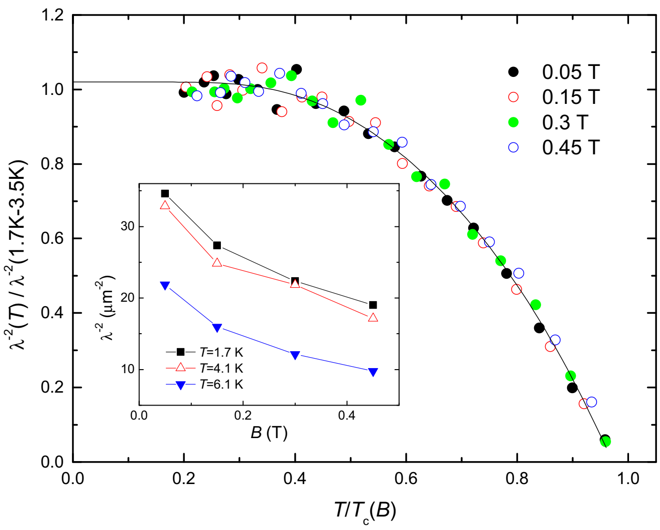

FIG. 3. (Color online) $\lambda^{-2}(T)$ normalized to its value averaged over the temperature range 1.7–3.5 K as a function of $T/T_c(B)$. The solid line is the fit obtained by using the weak-coupling BCS model [see Eq. (3)]. The inset shows the dependence of λ^{-2} on the applied field at $T = 1.7$, 4.1, and 6.1 K.

merge into the single line. The inset of Fig. 3 shows the field dependence of λ^{-2} for $T = 1.7$, 4.1, and 6.1 K.

First we will discuss the temperature dependence of λ^{-2}. It is seen that below approximately one half of T_c, λ^{-2} is temperature independent. The solid line in Fig. 3 represents a fit with the weak-coupling BCS model [36]:

$$\frac{\lambda^{-2}(T)}{\lambda^{-2}(0)} = \frac{\rho_s(T)}{\rho_s(0)} = 1 + 2\int_{\Delta(T)}^{\infty}\left(\frac{\partial f}{\partial E}\right)\frac{E\,dE}{\sqrt{E^2-\Delta(T)^2}}. \quad (3)$$

Here $\lambda^{-2}(0)$ and $\rho_s(0)$ are the zero-temperature values of the magnetic penetration depth and the superfluid density, respectively, and $f = [1+\exp(E/k_BT)]^{-1}$ is the Fermi function. The temperature dependence of the gap is approximated by $\Delta(T)/\Delta_0 = \tanh\{1.82[1.018(T_c/T-1)]^{0.51}\}$ [37], where Δ_0 is the maximum gap value at $T = 0$. The fit results in $\Delta_0(B)/k_BT_c(B) = 4.28(5)$, $\lambda^{-2}(T)/\lambda^{-2}(1.7$–$3.5\text{ K})=1.021(6)$, and $T/T_c(B) = 0.972(3)$. For $T_c(B=0) \simeq 8.4$ K (see Fig. 1) we get $\Delta_0(B=0) = 1.55(2)$ meV. Note that this value of the superconducting gap is close to $\Delta_0 = 1.85$ meV obtained from zero-field specific-heat data by Takayama *et al.* [6].

It is noteworthy that there is no need to introduce more than one gap parameter or to consider more complicated gap symmetry in order to satisfactorily describe $\lambda^{-2}(T)$ data. Fits using gap functions containing nodes result in higher χ^2 than that obtained for the simple s-wave gap model described above (see Sec. S3a in the Supplemental Material [8]). A fit using the anisotropic s-wave gap function results in χ^2 comparable to that of the s-wave model with an almost constant zero-temperature gap value ($1.50 \leqslant \Delta_0 \leqslant 1.60$ meV, see Sec. S3a in the Supplemental Material [8]). From the analysis of $\lambda^{-2}(T)$ data alone one could therefore conclude that $SrPt_3P$ is a a single-band s-wave superconductor. Note that a similar conclusion was reached by Takayama *et al.* [6] based on specific-heat data. In the following we will suggest that this was a premature conclusion obtained without considering the field dependence of λ.

As follows from the inset in Fig. 3, the field increase from 0.05 up to 0.45 T leads to the decrease of λ^{-2} by almost a factor of 2. In single-band s-wave superconductors, λ is *independent* of the magnetic field [32,37–39]. A dependence of λ on B is expected for superconductors containing nodes in the energy gap or/and multiband superconductors [33,38,40–42]. In the latter case the superfluid density within one series of bands is expected to be suppressed faster by the magnetic field than within the others [41,42].

The single s-wave gap behavior of $\lambda^{-2}(T)$ (see Fig. 3 and the discussion above) and the multiband features following after the upper critical field B_{c2} and $\lambda^{-2}(B)$ measurements (Figs. 1 and 2 and the inset in Fig. 3) reveal that $SrPt_3P$ is a *two-band* superconductor with energy gaps being *equal* within both bands [43]. Within a two-band model the deviation from the simple field independence of λ as well as the appearance of the upward curvature of the upper critical field could reflect the occurrence of two distinct coherence lengths ξ_1 and ξ_2 for two bands (associated with the corresponding upper critical field values $B_{c2,i} = \phi_0/2\pi\xi_i^2$) [35,41,42,44–46]. Following BCS, the zero-temperature coherence length obeys the relation $\xi \propto \langle v_F\rangle/\Delta_0$ (where $\langle v_F\rangle$ is the averaged value of the Fermi velocity). One could assume, therefore, that in $SrPt_3P$ the difference between ξ_1 and ξ_2 is caused by the different Fermi velocities ($\langle v_{F,1}\rangle \neq \langle v_{F,2}\rangle$), while the gaps remain the same ($\Delta_1 = \Delta_2$).

The statement about different $\langle v_F\rangle$'s in two Fermi surface sheets of $SrPt_3P$ is fully confirmed by the calculated band structure [7,9–11]. According to Refs. [7,9–11] there are two bands crossing the Fermi level having significantly different v_F's. The ratio of v_F's is, e.g., $\simeq 2$ along Γ-X and $\sim$3–4 along Γ-Z directions of the Brillouin zone. It is worth noting that different Fermi velocities on the different bands are expected to be a general feature of multiband superconductors as, e.g., MgB_2 [47–49], borocarbides [21,49], Fe-based superconductors [50,51], etc.

Note that the $SrPt_3P$ studied here is distinctly different from the "textbook" two-band superconductor MgB_2 in a particular way. In $SrPt_3P$ the charge carriers in both bands are expected to be almost equally strongly coupled to the phonons. Indeed, according to the band structure calculations of Nekrasov *et al.* [10] the carriers in two bands correspond to the relatively *similar* $pd\pi$ antibonding states of Pt(I)-P and Pt(II)-P ions, and are coupled to the *same* low-lying phonon modes confined to the *ab* plane. In contrast, in MgB_2 only the σ band carriers are coupled strongly to E_{2g} phonons, while the coupling of both, the σ and the π, bands to the harmonic B_{1g}, A_{2u}, and E_{1u} phonons is negligible [52]. Therefore, MgB_2 and $SrPt_3P$ correspond to two limiting cases of two-band superconductivity with the energy gaps being nonequal ($\Delta_1 \neq \Delta_2$, as in MgB_2) and equal ($\Delta_1 = \Delta_2$, as in $SrPt_3P$). At the same time $SrPt_3P$ remains the "true" two-band superconductor since, due to nonequal Fermi velocities ($\langle v_{F,1}\rangle \neq \langle v_{F,2}\rangle$), the carriers in various bands "respond" differently to the magnetic field [as shown here based on $B_{c2}(T)$ and $\lambda(B)$ studies and by Takayama *et al.* [6] based on the temperature dependence of the Hall resistivity].

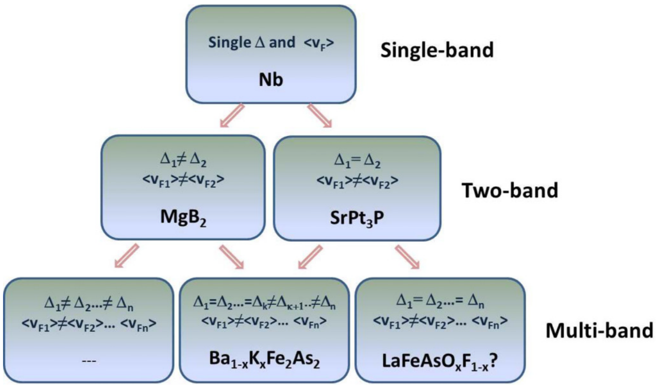

FIG. 4. (Color online) Schematic diagram representing relations between the various types of a single-band, two-band, and multiband superconductors.

By following the above presented arguments we propose a schematic diagram describing relations between the single-, two-, and multiband superconductivities (see Fig. 4). The single-band superconductor has essentially one gap value and one average Fermi velocity ($\langle v_F \rangle$). There are two types of two-band superconductors with energy gaps being equal ($\Delta_1 = \Delta_2$) or nonequal ($\Delta_1 \neq \Delta_2$). Both of these types are characterized, however, by nonequal $\langle v_F \rangle$'s. The way to multiband superconductors may proceed by different routes. (i) All gaps in all bands crossing the Fermi level are equal ($\Delta_1 = \Delta_2 \ldots = \Delta_n$). This is might be the case for the optimally doped $LaFeAsO_{0.9}F_{0.1}$ having five Fermi surfaces (as most other Fe-based superconductors, see, e.g., Ref. [1] and references therein). As shown by Luetkens *et al.* [53] the temperature evolution of the superfluid density of $LaFeAsO_{0.9}F_{0.1}$ is well described within the single s-wave gap approach, while λ^{-2} depends strongly on the magnetic field. It should be noted, however, that the presence of two distinct gaps in $LaFeAsO_{0.9}F_{0.1}$ was reported by Gonnelli *et al.* [54] based on the result of point contact Andreev reflection experiment. (ii) Gaps in some Fermi sheets are equal but in others are not ($\Delta_1 = \Delta_2 \cdots = \Delta_k \neq \Delta_{k+1} \cdots \neq \Delta_n$). A good example is the optimally doped $Ba_{1-x}K_xFe_2As_2$ where three gaps are equal ($\simeq$9 meV) while the last gap was found to be approximately eight times smaller ($\simeq$1.1 meV) [50,55]. (iii) Gaps in all the Fermi sheets are different ($\Delta_1 \neq \Delta_2 \cdots \neq \Delta_n$).

To summarize, the temperature and the magnetic field dependence of the magnetic penetration depth λ in the $SrPt_3P$ superconductor ($T_c \simeq 8.4$ K) were studied by means of muon-spin rotation. Below $T \simeq T_c/2$ the superfluid density $\rho_s \propto \lambda^{-2}$ is temperature independent which is consistent with a fully gapped superconducting state. The full $\rho_s(T)$ is well described within the single s-wave gap scenario with the zero-temperature gap value $\Delta_0 = 1.55(2)$ meV. However, λ was found to be strongly field dependent well below the upper critical field B_{c2}. This puzzle is reconciled by invoking a two-component model analysis with different characteristic length scales ξ_1 and ξ_2. To conclude, our results suggests that $SrPt_3P$ is a representative of a new class of multiband superconductors.

This work was performed at the Swiss Muon Source, Paul Scherrer Institut, Villigen, Switzerland.

[1] D. C. Johnston, Adv. Phys. **59**, 803 (2010).
[2] E. D. Bauer, F. Ronning, B. L. Scott, and J. D. Thompson, Phys. Rev. B **78**, 172504 (2008).
[3] F. Ronning, N. Kurita, E. D. Bauer, B. L. Scott, T. Park, T. Klimczuk, R. Movshovich, and J. D. Thompson, J. Phys. Condens. Matter **20**, 342203 (2008).
[4] K. Kudo, Y. Nishikubo, and M. Nohara, J. Phys. Soc. Jpn. **79**, 123710 (2010).
[5] S. Elgazzar, A. M. Strydom, and S.-L. Drechsler, J. Supercond. Novel Magn. **25**, 1795 (2012).
[6] T. Takayama, K. Kuwano, D. Hirai, Y. Katsura, A. Yamamoto, and H. Takagi, Phys. Rev. Lett. **108**, 237001 (2012).
[7] H. Chen, X.-F. Xu, C. Cao, and J. Dai, Phys. Rev. B **86**, 125116 (2012).
[8] See Supplemental Material at http://link.aps.org/supplemental/10.1103/PhysRevB.90.140507 for details of the upper critical field measurements, and the results of the analysis of the field and the temperature dependences of the magnetic field penetration depth.
[9] A. Subedi, L. Ortenzi, and L. Boeri, Phys. Rev. B **87**, 144504 (2013).
[10] I. A. Nekrasov and M. V. Sadovskii, JETP Lett. **96**, 227 (2012).
[11] C.-J. Kang, K.-H. Ahn, K.-W. Lee, and B. I. Min, J. Phys. Soc. Jpn. **82**, 053703 (2013).
[12] S. J. Williamson, Phys. Rev. B **2**, 3545 (1970).
[13] H. W. Weber, E. Seidl, C. Laa, E. Schachinger, M. Prohammer, A. Junod, and D. Eckert, Phys. Rev. B **44**, 7585 (1991).
[14] N. Toyota, H. Nakatsuji, K. Noto, A. Hoshi, N. Kobayashi, Y. Muto, and Y. Onodera, J. Low Temp. Phys. **25**, 485 (1976).
[15] D. Sanchez, A. Junod, J. Muller, H. Berger, and F. Levy, Physica B **204**, 167 (1995).
[16] M. Zehetmayer and H. W. Weber, Phys. Rev. B **82**, 014524 (2010).
[17] M. Zehetmayer, M. Eisterer, J. Jun, S. M. Kazakov, J. Karpinski, A. Wisniewski, and H. W. Weber, Phys. Rev. B **66**, 052505 (2002).
[18] A. V. Sologubenko, J. Jun, S. M. Kazakov, J. Karpinski, and H. R. Ott, Phys. Rev. B **65**, 180505 (2002).
[19] L. Lyard, P. Samuely, P. Szabo, T. Klein, C. Marcenat, L. Paulius, K. H. P. Kim, C. U. Jung, H.-S. Lee, B. Kang, S. Choi, S.-I. Lee, J. Marcus, S. Blanchard, A. G. M. Jansen, U. Welp, G. Karapetrov, and W. K. Kwok, Phys. Rev. B **66**, 180502 (2002).
[20] V. Metlushko, U. Welp, A. Koshelev, I. Aranson, G. W. Crabtree, and P. C. Canfield, Phys. Rev. Lett. **79**, 1738 (1997).
[21] S. V. Shulga, S.-L. Drechsler, G. Fuchs, K.-H. Müller, K. Winzer, M. Heinecke, and K. Krug, Phys. Rev. Lett. **80**, 1730 (1998).
[22] S. Manalo, H. Michor, M. El-Hagary, G. Hilscher, and E. Schachinger, Phys. Rev. B **63**, 104508 (2001).

[23] M.-A. Measson, D. Braithwaite, J. Flouquet, G. Seyfarth, J. P. Brison, E. Lhotel, C. Paulsen, H. Sugawara, and H. Sato, Phys. Rev. B **70**, 064516 (2004).
[24] F. Hunte, J. Jaroszynski, A. Gurevich, D. C. Larbalestier, R. Jin, A. S. Sefat, M. A. McGuire, B. C. Sales, D. K. Christen, and D. Mandrus, Nature **453**, 903 (2008).
[25] J. Jaroszynski, F. Hunte, L. Balicas, Youn-jung Jo, I. Raicevic, A. Gurevich, D. C. Larbalestier, F. F. Balakirev, L. Fang, P. Cheng, Y. Jia, and H. H. Wen, Phys. Rev. B **78**, 174523 (2008).
[26] S. Ghannadzadeh, J. D. Wright, F. R. Foronda, S. J. Blundell, S. J. Clarke, and P. A. Goddard, Phys. Rev. B **89**, 054502 (2014).
[27] A. Kortyka, R. Puzniak, A. Wisniewski, M. Zehetmayer, H. W. Weber, C. Y. Tang, X. Yao, and K. Conder, Phys. Rev. B **82**, 054510 (2010).
[28] T. B. Charikova, N. G. Shelushinina, G. I. Harus, D. S. Petukhov, V. N. Neverov, and A. A. Ivanov, Physica C **488**, 25 (2013).
[29] A. Yaouanc, P. Dalmas de Réotier, *Muon Spin Rotation, Relaxation and Resonance* (Oxford University, Oxford, 2011).
[30] A. Suter and B. M. Wojek, Phys. Procedia **30**, 69 (2012).
[31] E. H. Brandt, Phys. Rev. B **37**, 2349(R) (1988).
[32] R. Khasanov, I. L. Landau, C. Baines, F. La Mattina, A. Maisuradze, K. Togano, and H. Keller, Phys. Rev. B **73**, 214528 (2006).
[33] R. Khasanov, A. Shengelaya, A. Maisuradze, F. La Mattina, A. Bussmann-Holder, H. Keller, and K. A. Müller, Phys. Rev. Lett. **98**, 057007 (2007).
[34] E. H. Brandt, Phys. Rev. B **68**, 054506 (2003).
[35] S. Serventi, G. Allodi, R. De Renzi, G. Guidi, L. Romanò, P. Manfrinetti, A. Palenzona, Ch. Niedermayer, A. Amato, and Ch. Baines, Phys. Rev. Lett. **93**, 217003 (2004).
[36] M. Tinkham, *Introduction to Superconductivity* (Krieger, Malabar, FL, 1975).
[37] R. Khasanov, D. G. Eshchenko, D. Di Castro, A. Shengelaya, F. La Mattina, A. Maisuradze, C. Baines, H. Luetkens, J. Karpinski, S. M. Kazakov, and H. Keller, Phys. Rev. B **72**, 104504 (2005).
[38] R. Kadono, J. Phys.: Condens. Matter **16**, S4421 (2004).
[39] R. Khasanov, P. W. Klamut, A. Shengelaya, Z. Bukowski, I. M. Savič, C. Baines, and H. Keller, Phys. Rev. B **78**, 014502 (2008).
[40] M. Angst, D. Di Castro, D. G. Eshchenko, R. Khasanov, S. Kohout, I. M. Savič, A. Shengelaya, S. L. Bud'ko, P. C. Canfield, J. Jun, J. Karpinski, S. M. Kazakov, R. A. Ribeiro, and H. Keller, Phys. Rev. B **70**, 224513 (2004).
[41] A. Bussmann-Holder, R. Khasanov, A. Shengelaya, A. Maisuradze, F. La Mattina, H. Keller, and K. A. Müller, Europhys. Lett. **77**, 27002 (2007).
[42] S. Weyeneth, M. Bendele, R. Puzniak, F. Muranyi, A. Bussmann-Holder, N. D. Zhigadlo, S. Katrych, Z. Bukowski, J. Karpinski, A. Shengelaya, R. Khasanov, and H. Keller, Europhys. Lett. **91**, 47005 (2010).
[43] Our calculations presented in Sec. 3b in the Supplemental Material reveal that the maximum difference between two gaps does not exceed 15%.
[44] A. Gurevich, Phys. Rev. B **67**, 184515 (2003).
[45] R. Cubitt, M. R. Eskildsen, C. D. Dewhurst, J. Jun, S. M. Kazakov, and J. Karpinski, Phys. Rev. Lett. **91**, 047002 (2003).
[46] M. Mansor and J. P. Carbotte, Phys. Rev. B **72**, 024538 (2005).
[47] H. J. Choi, D. Roundy, H. Sun, M. L. Cohen, and S. G. Louie, Phys. Rev. B **66**, 020513 (2002).
[48] K. D. Belashchenko, M. van Schilfgaarde, and V. P. Antropov, Phys. Rev. B **64**, 092503 (2001).
[49] H. Suderow, V. G. Tissen, J. P. Brison, J. L. Martinez, S. Vieira, P. Lejay, S. Lee, and S. Tajima, Phys. Rev. B **70**, 134518 (2004).
[50] D. V. Evtushinsky, D. S. Inosov, V. B. Zabolotnyy, M. S. Viazovska, R. Khasanov, A. Amato, H.-H. Klauss, H. Luetkens, Ch. Niedermayer, G. L. Sun, V. Hinkov, C. T. Lin, A. Varykhalov, A. Koitzsch, M. Knupfer, B. Büchner, A. A. Kordyuk, and S. V. Borisenko, New J. Phys. **11**, 055069 (2009).
[51] A. Tamai, A. Y. Ganin, E. Rozbicki, J. Bacsa, W. Meevasana, P. D. C. King, M. Caffio, R. Schaub, S. Margadonna, K. Prassides, M. J. Rosseinsky, and F. Baumberger, Phys. Rev. Lett. **104**, 097002 (2010).
[52] T. Yildirim, O. Gülseren, J. W. Lynn, C. M. Brown, T. J. Udovic, Q. Huang, N. Rogado, K. A. Regan, M. A. Hayward, J. S. Slusky, T. He, M. K. Haas, P. Khalifah, K. Inumaru, and R. J. Cava, Phys. Rev. Lett. **87**, 037001 (2001).
[53] H. Luetkens, H.-H. Klauss, R. Khasanov, A. Amato, R. Klingeler, I. Hellmann, N. Leps, A. Kondrat, C. Hess, A. Kohler, G. Behr, J. Werner, and B. Büchner, Phys. Rev. Lett. **101**, 097009 (2008).
[54] R. S. Gonnelli, D. Daghero, M. Tortello, G. A. Ummarino, V. A. Stepanov, J. S. Kim, and R. K. Kremer, Phys. Rev. B **79**, 184526 (2009).
[55] R. Khasanov, D. V. Evtushinsky, A. Amato, H.-H. Klauss, H. Luetkens, Ch. Niedermayer, B. Büchner, G. L. Sun, C. T. Lin, J. T. Park, D. S. Inosov, and V. Hinkov, Phys. Rev. Lett. **102**, 187005 (2009).